OXFORD JOURNAL
OF STUDENT
SCHOLARSHIP

Design of an Adaptive Joystick Console with Active Force Feedback and Tremor Filtering for Accessible Vehicle Control

Gouransh Sethi
gouraanshsethi@gmail.com

ABSTRACT

Single-lever joystick controls are the main method of independent driving for individuals with tremor, quadriplegia, or limited mobility in their legs, and although several systems have been reviewed, none include adaptive per-user profiling, frequency-selective tremor filtering and input-conditioning provisions for unintended transient commands, active force feedback, proximity sensing, rapid mode switching, and fatigue-reducing ergonomics in a single console. Three of the commercial systems, Maya Mobility 4-Way Joystick, Joysteer 3.0 and EMC AEVIT 2.0 were reviewed and redesigned based on the literature; three research programmes, J4D, an HFES-Europe study, a research wheelchair-integrated drive system were evaluated on a rubric of seven criteria, where 8 consolidated faults were identified and mapped to fixes. Five EV gearbox architectures and six gear-selector mechanisms were compared in a parallel study to determine if the gear selector should be in the console. Six changes were quantified and made in the revision from Iteration 1 to Iteration 2: an arc of ±25° in the travel range, an indicator ring for haptic feedback, auxiliary buttons moved 15 mm towards the center, a recessed guarded emergency stop, a 40 × 20 mm status display, and a mounting bracket that was expanded 30 mm on each side. No measurements were taken, and performance targets were derived analytically. Analytical frequency-response calculations for the proposed second-order low-pass stage predict an attenuation of about 6-24 dB for the 3 Hz low-speed cutoff for 4-12 Hz, with higher cutoff at higher vehicle speed, reducing the attenuation. These values are not measured values of tremor suppression; instead they are calculated values of filter response. Single-speed was given more points for weighted scoring, and the joystick-integrated gear selection was only seen as viable with detent feedback. All values are unvalidated targets that need to be used while benchmarking and on-road testing.

Keywords: Assistive driving technology; Joystick control systems; Human–machine interface (vehicle accessibility); Force feedback and haptics; Tremor filtering; Adaptive mobility devices; design science; shift-by-wire

1. INTRODUCTION

Traditional car controls contain suppositions regarding the body that operates them. A standard steering wheel requires approximately 900° of rotation between the lock and unlock positions; low-speed manoeuvring requires a hand-over-hand grip position, a full range of shoulder motion, and torques between several N·m (Bhise 2011). Pedal operation assumes independent control of the lower limb. Every assumption corresponds to a separate population: tremor and spasticity cause loss of fine positional control, a loss of grip strength is the effect of the torque requirement, and a quadriplegia eliminates the movement envelope (El-Sheikh et al., 2025). The result is not only a hassle, but it is also a loss of transportation, which is integral to jobs, health care, and independence.

The industry standard engineering solution is single-lever joystick control. The commercial adoption of the Maya Mobility 4-Way Joystick System, Joysteer 3.0, and EMC AEVIT 2.0 confirms that steering, acceleration, and braking can be combined into a single lever in a certified drive-by-wire system. The results are confirmed by research programmes: the J4D Project has trained severely disabled drivers to drive an adapted vehicle for licensing, and a 16-driver on-road trial has been conducted with participants with cervical spinal-cord injury using a force feedback system with decoupled steering (PETERS & OESTLUND, 2026).

The paradigm is thus possible but not realized. The six capabilities cited above are those that are present in the reviewed corpus, but never occur in more than one at a time: adaptive per-user calibration, software-level tremor and spasticity filtering, active force feedback, proximity sensing, rapid switching between accessible and conventional controls, and ergonomics used to reduce fatigue. None of the reviewed accessibility systems address gear selection, even though there have been documented instances of rolls away caused by having ambiguous electronic selectors.

This paper proposes a console that fills all six gaps based on an Iteration 1 to Iteration 2 redesign, and responds to two research questions:

RQ1: Is it possible to add both active force feedback and tremor filtering to a single lever console, without reinvoking the same fatigue and precision compromises found in the J4D and HFES-Europe studies?

RQ2: Is the inclusion of gear selection in the joystick less likely to create the inherent gear-state risk that has been described for rotary-mounted and push-button shifters?

The contribution is a design specification that outlines a fault and specifies analytically derived performance metrics, a quantified gap-coverage comparison to the reviewed corpus, and an explicit account of the trade-offs that each of the fixes entails. No measure is ever reported anywhere, and all derived values are referred to as targets.

2. MATERIALS AND METHODS

2.1 Study design

This is not an empirical trial, but a design-science study. It goes through four stages: (i) structured review of prior art, (ii) fault derivation and consolidation, (iii) iterative design revision using traceability between faults and fixes, and (iv) analytical derivation of performance targets. There was no human involvement and no physical prototype tested. All the numerical results mentioned in Section 3 are either taken from the literature or calculated from first-principles vehicle-dynamics, signal-processing, and control calculations explicitly outlined in Sections 2.6–2.8. Design targets are derived values. They're not measurements; they're not a prediction of measured performance.

2.2 Source corpus and inclusion criteria

Sources that claimed (a) a single-lever or reduced-effort primary control (b) ergonomic or safety data associated with gear selection or (c) efficiency data for an electric-vehicle transmission architecture were admitted. Four categories were put together.

Commercial systems: Maya Mobility 4-Way Joystick System, Joysteer 3.0 (Steering Developments, UK; certified to ECE R79/R13/R10) and EMC AEVIT 2.0 (USA). (Steering Developments, 2026, *AEVIT™ 2.0 System Overview*, 2022)

Research systems: J4D (Joystick for Driving) Project, ONCE Foundation and Universidad Politècnica de Valencia, 2012–13; a force-feedback, decoupled-steering trial, with 16 drivers with cervical spinal cord injury (PETERS and OESTLUND 2026) and a joystick car drive system without seat transfer (Wada & Kameda, 2009) .

Patent literature: WO 2005/120929 (unintentional joystick actuation); US 7,970,514 (force feedback for disabled drivers); US 4,722,416 (hydraulic one-limb accelerator/brake); EP 1,595,766 (potentiometer-based sidestick).
Drivetrain and selector sources: single-speed, two-speed, AMT, DCT, and CVT (Lacock et al. 2023; Ruan et al. 2016; 2018); mechanical, rotary, column-stalk, push-button, joystick-type, and touchscreen selectors (Lohilahti Bladfält et al., 2020); NHTSA investigation data for rollaway and other issues (*Rollover Data Special Study: Final Report*, 2011) .

There are two exclusions that are pertinent to interpretation. First, there are no peer-reviewed sources for commercial grade; capability claims and, critically, capability absences are based on vendor documentation, which is not an exhaustive specification. Second, there are no source reports of controlled comparative trials of the specific fixes proposed here.

2.3 Fault derivation protocol

Faults were obtained in four stages.

1. ***Feature extraction*.** Control degrees of freedom, feedback modality, calibration method, safety interlocks, sensing, mode switching mechanism, and installation dependency were coded for each system.

2. ***Deficiency coding*.** All explicit deficiency statements in a source and all capabilities not mentioned in the schema were captured as candidate faults with the source reference.

3. ***Consolidation.*** Candidates with similar causal mechanisms for their faults were combined into a single fault. (Table 2).

4. ***Fix mapping.*** All consolidated faults are mapped to a single design intervention, with no fault being left uncorrelated to an Iteration 2 change and none being left unaddressed.

Coding was performed by a single analyst. No inter-rater reliability was obtained, which is reported as a threat to validity in Section 4.9. A single analyst carried out the fault identification, evidence coding and comparative classification. There was no second rater assessment for independence and thus inter-rater agreement cannot be reported.

2.4 Comparative evaluation rubric

For the use case of accessibility-retrofit, gearbox architectures and selector mechanisms were evaluated using an ordinal scale of 1–5 (with 5 being the most favourable) with explicit anchors. Weighting is based on the design principle that, in this user base, if the system is not reliable or complex, it is not only expensive but it is also unsafe, because the user may not be able to intervene manually.

***Gearbox criterion weights*:** reliability 0.25, complexity 0.20, cost 0.15, maintenance 0.15, efficiency 0.15, torque delivery 0.05, ergonomics 0.05.

***Selector criterion weights*:** blind/tactile operability 0.25, one-hand and limited-range-of-motion operability 0.20, error-rate evidence 0.20, reliability 0.15, package space 0.10, cost 0.10.

For transparency, each criterion was scored independently using the stated ordinal scale before multiplication by its assigned weight.

Weighted totals were calculated as $S = \sum w_i s_i$, where w_i is the criterion weight and s_i is the criterion score. The final weighted totals are not the only criterion scores that are reported, they are presented as a full set of scores. As the weights are based on analysis and not user preference, an equal-weight sensitivity calculation was also conducted to check the robustness of the qualitative ordering with respect to the choice of weights.
Weights were set a priori by the design premise, not tuned to the result.

2.5 Iterative design process

The baseline architecture established in Iteration 1 comprised single lever steering, acceleration and braking, twin proportional trigger paddles, a 6-button auxiliary arc on an R50 mm radius, a proximity-sensor housing, a Ø48 mm emergency stop and a 120–210 mm telescoping mounting arm that ended in a wheelchair armrest clamp. The joystick height is 140 mm, the console body's height is 45 mm, the mounting arm is Ø32 mm, and the console's head has a diameter of 115 mm in a 160 x 160 mm footprint.

Table 1. Changes applied by Iteration 2, each traceable to a fault

	Change	Fault addressed	Mechanism
1	Travel arc capped at ±25°	F1, F2	Removes arm rotation; enables wrist-only actuation
2	Haptic feedback indicator ring at joystick base	F4	Visual confirmation of force-feedback state
3	Auxiliary buttons repositioned 15 mm inward (R50 → R35 mm)	F1	Reduces lateral reach for limited range of motion
4	Emergency stop recessed with raised guard rim	F3	Prevents actuation by involuntary movement
5	40 × 20 mm digital status display added	F4, F8	Displays applied force, speed, proximity state
6	Mounting bracket widened 30 mm per side	F7	Fits wider wheelchair armrests without custom parts

2.6 Analytical derivation of steering targets

The main challenge of the console is the angular compression, with a ±25° stick having to span the authority of a wheel with ±450° movement, which is a compression ratio of 18:1. This results in either insufficient low-speed authority or unsuitability of high-speed sensitivity under this fixed gain. A gain was thus obtained over a speed-scheduled time.

Road-wheel angle δ is mapped from stick angle θ by

$$\delta(\theta, v) = k(v) \cdot \theta, \quad \text{where } k(v) = k_{min} + (k_{max} - k_{min}) \cdot e^{(-v/v_0)}$$

with k_max = 1.40 °/° (full stick → 35° road wheel at rest, giving a 3.9 m minimum turn radius for a 2.7 m wheelbase), k_min = 0.09 °/°, and v_0 = 22 km/h.

The lateral acceleration at full deflection has been tested using the linear bicycle model, and

$$a_y = v^2 \cdot \delta / [L \cdot (1 + K \cdot v^2)]$$

for wheelbase L = 2.7 m and understeer gradient K = 0.0024 s²/m².

For a specified target lateral acceleration $a_{y,target}$, rearranging the model gives the corresponding road-wheel angle as

$$\delta(v) = \frac{a_{y,target} L(1+Kv^2)}{v^2}.$$

This expression is used as a theoretical benchmark to compare the chosen exponential gain schedule. The schedule used here is an approximation in the design, and is not the one and only solution to the lateral-response problem.

Other important design considerations for a complete steering-controller design would involve assessing yaw-rate response, transient behaviour, tyre nonlinearities, actuator dynamics, and stability margins, and are not within the scope of the current analytical study (Li et al., 2026).

The results are presented in Table 6. The constants k_min and v_0 were determined so that lateral acceleration is constant when the stick is fully deflected (lateral deflection = ±100%) above 40 km/h, that is, when the physical meaning of stick deflection is the same for all speeds.

2.7 Tremor filter design and latency budgeting

The frequencies of voluntary steering input are found to be below about 2 Hz, while those of pathological tremor are found to be in the range of 3-12 Hz (cerebellar and intention tremor 3-5 Hz, Parkinsonian rest tremor 4-6 Hz, essential tremor 4-12 Hz, and physiological tremor 8-12 Hz) (Lenka & Jankovic, 2021; Bhatia et al., 2017). Tremor-suppression approaches reported in the clinical-engineering literature are predominantly wearable or orthotic (Bhidayasiri et al. 2022; Mo and Priefer 2021) whereas the present design filters the control signal itself. The adaptive dead zone is used around the neutral position of the joystick and is designed to help reduce minor unwanted movements when trying to input a neutral movement. It will not suppress tremor which is superimposed on a steady non-zero voluntary command. The frequency-selective low-pass/notch stages are instead used to deal with tremor during steering. Besides, the upper reported tremor excursion of 3.2° which is used in this case, is larger than the upper estimation of the dead zone, about 3°, so the dead zone cannot be expected to exclude the whole range of unwanted inputs.The three-stage cascade was defined as:

1. ***Adaptive dead zone.*** Width set per profile at 8–12% of the ±25° arc, i.e., 2.0–3.0°. Sizing is based on the tremor excursion at the grip, which is 1.9–3.2° from the gimbal's pivot with an effective grip radius of 90 mm from the pivot. The 3.0° dead zone thus, in turn, allows displacements up to 4.7 mm.

2. ***Second-order Butterworth low-pass filter***, cutoff frequency of f_c = 3.0 Hz below 30 km/h, and then increases to 6.0 Hz above 80 km/h. Magnitude response $|H(f)| = 1/\sqrt{(1 + (f/f_c)^4)}$. Group delay at DC, $\tau = 2\zeta/\omega_n = \sqrt{2}/(2\pi f_c)$, gives 75 ms at 3 Hz and 37 ms at 6 Hz.

3. ***Adaptive notch*** tracking the dominant spectral peak in the band 3 - 12 Hz with the specified rejection level of ≥20 dB and negligible off-band delay. When reliable estimation of tremor frequency is not available and/or the adaptive frequency is outside the allowed frequency range of

3–12 Hz, the adaptive notch is not allowed to follow the unconstrained frequency. The signal-processing chain is returned to the bounded deterministic architecture, however. This fall-back is defined as a safety requirement and experimental validation of this fall-back is not achieved in the present study.

The longest analytical pipeline is for the low-speed 3 Hz filter configuration. A latency of about 143 ms is equivalent to the travel of about 1.19 m of the vehicle at the top of the range of the intended low speed region (30 km/h). The high speed filter configuration has a lower calculated filter delay, due to its higher cutoff. A compromise between rejection and latency at high speed is therefore a design decision, and will be discussed in Section 4.5.

Most importantly, filtering becomes asymmetric; it only applies to the input path. The output path of the force feedback is set to 100 Hz, as trying to lower the road force feedback to 3 Hz would negate the need to feed back at all. An end-to-end latency budget was built up by adding each stage with a ceiling of ≤150 ms (Table 7). The aim of the frequency selective filtering architecture is to mainly filter oscillatory tremor. The adaptive notch filter is not assumed to reduce the spasticity because it is not assumed to be a periodic disturbance, like tremor. Disturbances that do not oscillate would need to be dealt with differently, for example using bounded rate limiting or transient-input detection. It is not assessed in the present analytical study how effective they are.

2.8 Force-feedback sizing and the strength-conflict constraint

The reviewed literature does not address the conflict of how the console can be light enough to be moved by a user with lowered strength and yet be resistant enough to provide the user with a sense of road state (PETERS and OESTLUND 2026). An absolute 15 N maximum may be greater than a voluntary capability of the intended user as specified in Iteration 1.

So the ceiling for feedback was redefined as a relative quantity:

$$F_{fb,max} = 0.40 \times F_{MVC}$$

F_MVC is the user's maximum voluntary force at the grip, during the profile setup procedure. A user with 20 N voluntary capability can use only 8 N. The absolute range of 0-15N is only kept for the design envelope of the actuator.

Additionally, the centering stiffness is limited by the user-relative force limit. Therefore, the commanded centering force at any joystick displacement should be controlled to meet the requirement Fc()Flimit, with Flimit being the measure of the user's voluntary force capability. The quoted stiffness range then is not a force that the user must experience with the actuator, but rather a stiffness envelope for the actuator/design. The stiffness command should be lowered for users who have lower measured force capability." The chosen 0.40 FMVC ceiling is considered a provisional upper ceiling design limit, rather than a validated sustained ergonomic limit. The tolerance of sustained forces will need to be validated with the user for future use. Actuator torque follows from the 90 mm grip radius: 15 N × 0.09 m = 1.35

N·m per axis. The centring stiffness can be adjusted between 12 and 45 N·mm/deg, providing a full deflection of 3.3 N to 12.5 N.

2.9 Gear-selection assessment method

Comparative simulation (CS) ergonomic preference and error-rate data were used to evaluate the RQ2 question for all three evidence streams: (i) ergonomic preference and error-rate data from comparative simulation; (ii) real-world incident data (NHTSA rollaway reports on rotary shifters) ("Rollover Data Special Study: Final Report," 2011) ; and (iii) the weighted selector rubric of Section 2.4. When preference and error-rate data conflict, both are given; no effort has been made to reconcile the two in a single verdict without being explicit about the conflict. There is a safety interlock specified for integrated gear selection function. A gear selection command is only accepted if (i) the measured vehicle speed is zero, (ii) the service brake is applied and (iii) the user has selected gear selection mode. Input to gear selection is blocked during normal vehicle motion. After a successful selection the engaged state is shown continuously and verified by a distinct feedback signal.

2.10 Figure production

Figures 1–3 are CAD sketches and renders, created in Autodesk Fusion 360 and reproduced in Section 3.1. The dimensions given in Section 3.1 are nominal design dimensions and not manufactured tolerances and are taken from the figure annotations. The figures are the primary record of the Iteration 1 to Iteration 2 change set, and each one was audited against the other two and against the change list, with any discrepancies reported.

3. RESULTS

3.1 Design geometry and figure description

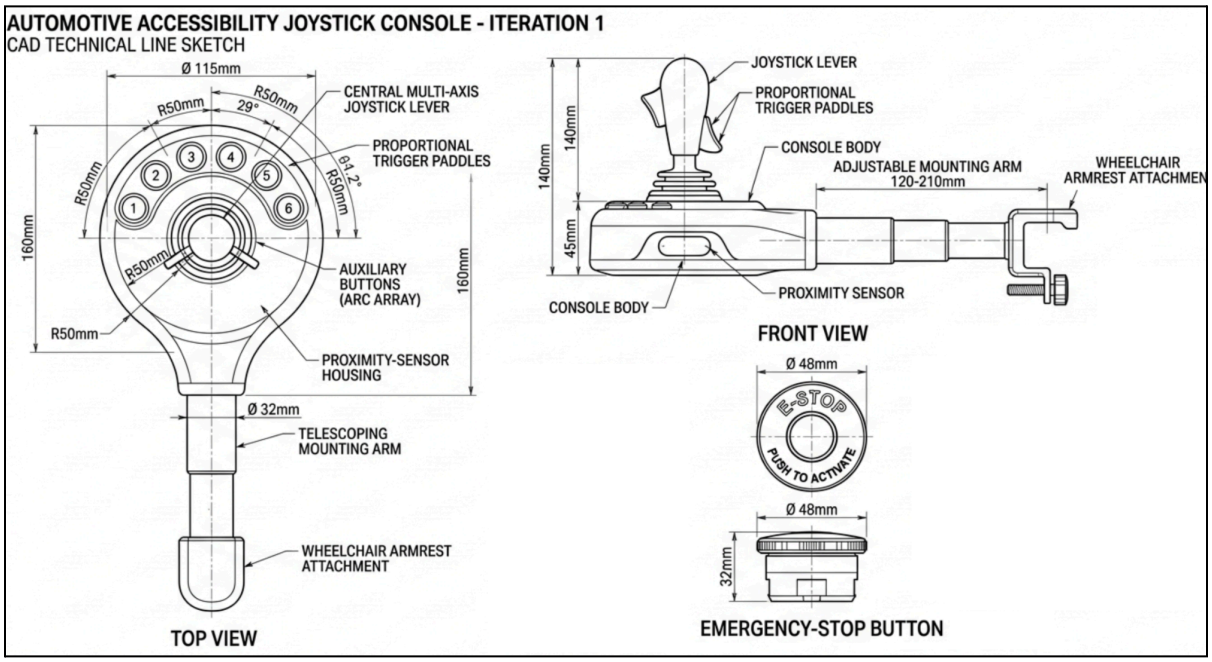


Figure 1. Iteration 1 three-view technical sketch (top, front).

The envelope measures Ø160 and the console-foot is a circular head, with a diameter of Ø115 mm, and a multi-axis joystick lever in the middle. Six buttons are equally spaced apart by 29° and there is a total of 145°. The arc length for this is about 126.5 mm for R=50 mm and 88.6 mm for R=35 mm, which is about 30% less of the total arc which would contain the button centres. But it also means that the arc spacing between each button (center to center) is reduced from approximately 25.3 mm to 17.7 mm, when the radius is reduced from R=50 mm to R=35 mm. The inward move to the new location will shorten the reach required, but may increase the likelihood of activation of adjacent buttons. The design target of R=35 mm has been retained as a result of the absence of ergonomic user testing, and is not necessarily a spacing that is ergonomically optimal. The proximity-sensor housing is in front of the console body, and a Ø32 mm telescoping arm extends from the console body to the wheelchair armrest attachment. The front view has an overall height of 140 mm above the console body (which is 45 mm); the adjustable arm measures 120–210 mm. Another detail depicts the surface-mounted Ø48 mm emergency stop that is situated at 32 mm height. The isometric image fixes the two trigger paddles that are positioned on either side of the trigger lever as well as the numbering order of the auxiliary buttons 1–6. It is not stated that an emergency control will remove steering or braking authority if it is activated while the vehicle is moving. Rather, this triggers a demand for a controlled minimal risk response, while maintaining the control functions necessary to ensure vehicle stability. The response of the vehicle itself depends on the host drive by wire architecture and is host dependent and needs to be analysed from a functional safety perspective..

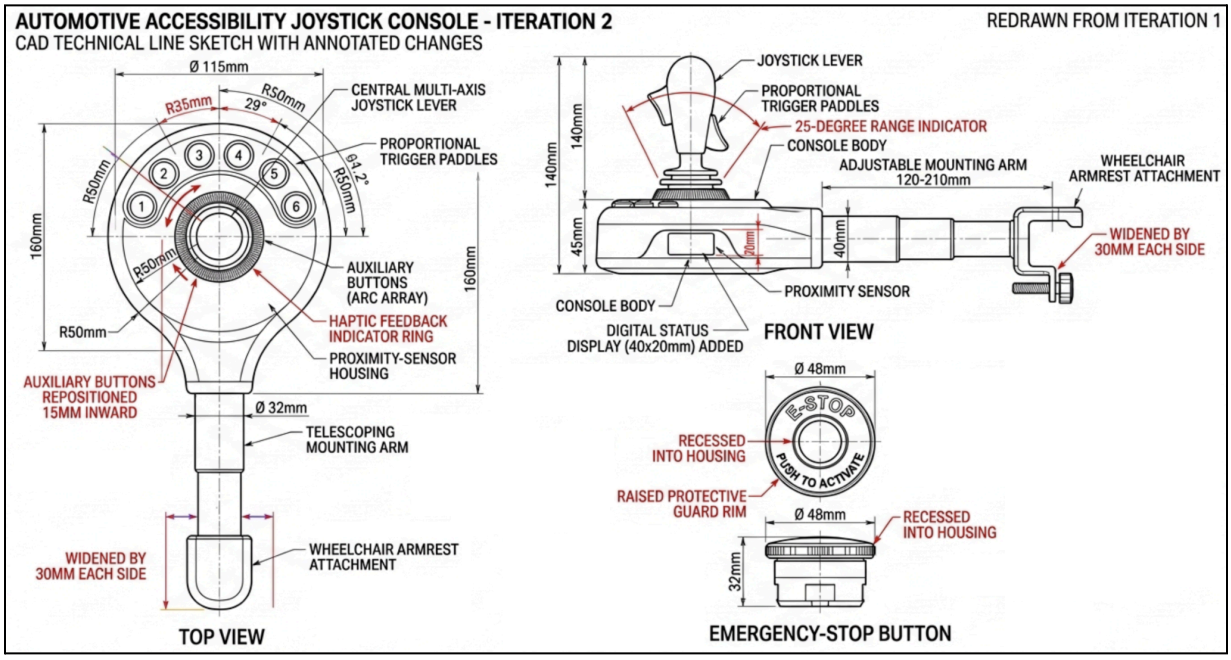


Figure 2. Iteration 2 redesign with annotated difference callouts. Figure 2 is drawn directly on top of the Iteration 1 geometry, with changes indicated in red so that the changes can be seen visually. There are 6 differences shown and explained. A repositioning of R15 mm towards the center of the auxiliary button arc is achieved in its repositioning, from R50 mm to R35 mm. The front view now has a 25-degree window that indicates the range of view. This is not a reduction, but a new limit, as Iteration 1 calls for no travel arc and the 29° dimension remains in both top views, which is the button pitch. A concentric haptic feedback indicator ring is added to the bottom of the joystick. The emergency stop, which has a diameter of Ø 48 mm, is embedded in the enclosure behind a raised protective guard rim; no actuating surface is required, unlike that shown in Figure 1. A 40 × 20 mm digital status display is integrated into the console body face - the red 20 mm dimension indicates that it is packaged within the unaltered 45 mm body height, not making it larger. The armrest attachment of the wheelchair is widened by 30 mm on each side, thus increasing the total span by 60 mm.

The following are three geometric results that are quantified directly from Figures 1 and 2:

- ***Travel arc*:** capped at ±25° in Iteration 2. No travel-arc annotation is on Iteration 1, so this is a new constraint, not a reduction from a previous value.
- ***Reach reduction:*** the button arc length of the 6-button span is reduced from 126.5/127 mm (πR at R50) to 88.6/89 mm (πR at R35), thus reducing the traverse distance by 30.0%.
- ***Packaging:*** A 40 × 20 mm display fits into 20 mm of the 45 mm body face and fits within without raising the body height. The Iteration 2 change set thus does not affect the dimensional regression.

Figures 1-2 were prepared using Fusion360 software.

3.2 Comparative system overview

Table 2. Reviewed commercial, research, and patent systems.

System	Type	Key capability	Critical limitation (as reported)
Maya Mobility 4-Way Joystick	Commercial	Single lever, servo-assisted, all primary functions	Four-direction movement only; no haptics; minimal customisation
Joysteer 3.0 (Steering Developments 2026)	Commercial	Drive-by-wire; ECE R79/R13/R10 certified; modular inputs	High cost; specialist-only installation; complex setup
AEVIT 2.0 (Electronic Mobility Controls 2022)	Commercial	Flash-upgradeable; joystick plus touchscreen	Proprietary; vehicle-specific; few certified installers
J4D Project (PETERS and OESTLUND 2026)	Research	Simulator plus adapted vehicle for severe disability	Elevated mental workload; stress and fatigue on long drives
Joystick car drive, wheelchair-integrated (Wada and Kameda 2009)	Research	Mechanical failsafe; DC-motor steering	Rigid coupling; no adaptive feedback; bulky
Hydraulic controller, US 4,722,416	Patent	Hydraulic accel/brake; one-limb operation	Complex mechanics; no electronic precision
Sidestick system, EP 1,595,766	Patent	Potentiometer-based; electric-motor link	Not user-adjustable; passive feedback only
Vehicle for disabled people, US 7,970,514	Patent	Force-feedback provision	Feedback not adaptive to user strength

3.3 Consolidated fault-to-fix matrix

Table 3. Eight consolidated faults with supporting evidence and mapped fixes.

	Fault	Evidence	Fix
F1	Driver fatigue from arm-wide movement	Full-arm rotation required by reviewed systems; J4D reported elevated workload and stress in city driving	Wrist-only 25° arc, ergonomic palm rest, adjustable arm support

F2	Cross-axis steering/speed interference	Joystick angular range approximately 1/30 of a wheel's; rapid steering bleeds into unintended acceleration	Independent per-axis sensitivity curves plus a calibrated 2 × 2 decoupling matrix
F3	Unintentional actuation	Tremor, spasticity, and road vibration register as input; hazard documented in WO 2005/120929	Adaptive deadzone, median outlier rejection, low-pass and adaptive-notch filtering
F4	Absent or passive force feedback	Road surface, grip limit, and lateral-G information lost; passive-only in EP 1,595,766	Active haptic actuator, output rendered to 100 Hz, ceiling scaled to measured user strength
F5	Non-adaptive calibration	Systems fixed at manufacture; cannot track strength, range of motion, or condition progression	Five stored digital profiles: force threshold, deadzone, gain, stiffness, feedback ceiling
F6	Slow mode switching	Reverting to conventional control requires hours of mechanical servicing, blocking shared or emergency use	User-initiated changes between command mappings/control modes are inhibited while the vehicle is moving. Profile loading or mode changes that alter steering, acceleration, or braking mappings require a stationary vehicle state.
F7	Cost and proprietary lock-in	Joysteer and AEVIT require specialist, vehicle-specific installation; few certified installers	Universal mounting bracket, open calibration interface, CAN-standard signalling
F8	No proximity sensing	No reviewed system integrates low-speed obstacle/proximity awareness	Four-sensor ultrasonic array, 0.3–5 m, tiered audible and haptic alerts

3.4 Gap-coverage comparison

All systems were rated on a 0-2 scale (0 - none, 1 - some, 2 - present) for each of the six target capabilities and gear integration (maximum 14).

Table 4. Evidence and design-requirement traceability across reviewed systems

System	Adaptive profiling	Tremor filtering	Active feedback	Proximity	Fast mode switch	Wrist ergo-nomics	Gear integrati on	Total	%
Maya 4-Way	0	0	0	0	0	1	0	1/14	7.1
Joysteer 3.0	1	0	1	0	1	1	0	4/14	28.6
AEVIT 2.0	1	0	0	0	1	1	0	3/14	21.4
J4D Project	1	0	1	0	0	0	0	2/14	14.3
Wheelchair joystick	0	0	0	0	0	1	0	1/14	7.1
US 7,970,514	0	0	2	0	0	0	0	2/14	14.3
EP 1,595,766	0	0	0	0	0	0	0	0/14	0.0
US 4,722,416	0	0	0	0	0	0	0	0/14	0.0
Proposed Iteration 2	**2**	**2**	**2**	**2**	**2**	**2**	**1**	**13/14**	**92.9**

Existing systems: entries reflect the evidence found in the documents reviewed. In the proposed system, entries are limited to showing if the capability is a part of design specification. It is, therefore, not the same as demonstrated implementation or performance, but rather a 'specified' entry.

3.5 EV gearbox architecture comparison

Table 5. Comparative summary of EV gearbox technologies, with weighted accessibility score.

Parameter	Single-speed	Two-speed	AMT	DCT	CVT
Efficiency	High at low/mid speed; falls at highway speed	~94% typical; 7–11% energy saving vs single-speed	Driveline loss; better only at very high speed	Up to 14% motor efficiency gain	Comparable to DCT; smoother delivery
Torque delivery	Continuous, uninterrupted	Brief shift interruption	Interruption during clutch shift	Near-seamless, pre-selected	Continuous, stepless
Cost	Lowest	Moderate high	Moderate	High	High

Complexity	Lowest	Moderate	Moderate–high	High (dual clutch packs)	High (belt/variator)
Maintenance	Minimal	Low moderate	Moderate (clutch wear)	Higher	Moderate (belt wear)
Range impact	Baseline	Up to 4.2% improvement, NEDC	Marginal or negative net gain	Up to 15% energy saving	Similar to DCT
Typical application	Mass-market passenger EVs	Performance and luxury EVs	Heavy commercial EVs, buses	High-performance, heavy-duty	Premium passenger EVs
Weighted score (max 5.00)	**4.70**	**3.75**	**2.75**	**2.90**	**3.00**

It leads its closest competitor by 0.95 points. The margin is almost solely determined by the reliability and complexity criteria, which add up to 0.45 weight. While the gains in efficiency available from multi-speed designs are real (4-15%), they are not enough to change the ranking when weighted by accessibility (Lacock et al. 2023; Ruan et al. 2018; 2016).

3.6 Gear-selector mechanism comparison

Table 6. Selector mechanism comparison with weighted accessibility score.

Selector	Principle	Advantage	Disadvantage	Reliability evidence	Weighted score
Mechanical lever (PRNDL)	Cable or linkage directly to transmission	Tactile, familiar, position hard to misread	Bulky; consumes console space; requires arm travel	High; few failure points	3.80
Rotary dial (shift-by-wire)	Dial position signals gear electronically	Compact; frees console space	Documented driver confusion over gear position	The cited NHTSA investigation recorded 1,448 complaints, including 684 crashes, 149 injuries, zero fires, and one fatality,	2.55

				involving approximately 1.28 million vehicles. These data describe reported incidents associated with the investigated selector/vehicle population and should not be interpreted as an experimentally determined error rate for rotary selectors in general.	
Column stalk	Electronic shift from column-mounted stalk	Frees console; near-wheel single-hand use	Confusable with wiper and indicator stalks	High in modern implementations	3.55
Push-button (PRND)	Momentary buttons to shift-by-wire unit	Very compact; fast selection	No tactile sweep; needs visual confirmation	High; solid-state	3.45
Joystick-type	Spring-loaded multi-directional stick to TCU	Single-hand, small-range operation; polystable joysticks had the highest usability of the types tested (Lohilahti Bladfält et al. 2020)	Monostable (spring-return) joysticks less efficient, harder to use and more sensitive to reduced visibility (Lohilahti Bladfält et al. 2020); unfamiliar layout	Good; few moving parts, Monostable joystick-type shifter recalled: 811,586 vehicles, 266 crashes, 68 injuries (NHTSA 2016)	3.80

Touchscreen	Software selection via infotainment	Fully reconfigurable; no hardware	Requires visual attention; no tactile feedback; single point of failure	Dependent on screen and software	2.05
Proposed: joystick with haptic detents	Stick selection with detented force feedback and display confirmation; standstill interlock; automatic Park	Retains single-hand operability; restores tactile confirmation during selection	Unvalidated; adds actuator dependency to the gear path; monostable by necessity (stick re-centres to steer)	Target only, no data	3.85

There is no physical implementation or evaluation of the proposed selector that has been used to measure errors of selection. Therefore, there is no evidence that haptic detents, the persistence of gear indications, and mode interlocks are intended to reduce errors, and they are not tested as such. It is not claimed that the proposed selector has any comparative error-rate advantage.

Mechanical lever and joystick type selectors are rated at a 3.80 on the accessibility-weighted rubric, but for different reasons. The mechanical lever is rated 5 in terms of tactile confirmation, 2 in terms of operability with one hand, and the joystick is rated 5 in terms of operability and 2 in terms of evidence of error rate. For the target population, the lever's weakness disqualifies it; the joystick's weakness is addressed by design for the target population. The weighted assessment does not prove the real world selector performance, it only shows the characteristics which are prioritized in the proposed concept. Especially, the development of user error criterion, reliability criterion and tactile effectiveness criterion must be physically developed and empirically validated.

3.7 Derived steering gain schedule and lateral-acceleration normalisation

Table 7. Speed-scheduled steering gain and resulting full-deflection vehicle response.

Speed (km/h)	**Gain k (°/°)**	**Road-wheel angle at ±25° stick**	**Lateral acceleration at full deflection (m/s²)**	**(g)**
0	1.400	35.0°	-(3.86 m turn radius)	-

Speed (km/h)	Gain k (°/°)	Road-wheel angle at ±25° stick	Lateral acceleration at full deflection (m/s²)	(g)
10	0.922	23.0°	1.13	0.115
20	0.618	15.4°	2.87	0.292
30	0.425	10.6°	4.09	0.417
40	0.303	7.6°	4.66	0.475
60	0.176	4.4°	4.73	0.482
80	0.125	3.1°	4.55	0.464
100	0.104	2.6°	4.54	0.463
120	0.096	2.4°	4.68	0.477

The schedule has almost constant full-deflection lateral acceleration ranging from 0.46 g to 0.48 g, a variation of 4.1% between these two values. The speed-dependent gain schedule is a design law made up of the chosen vehicle-model parameters and the goal of reducing lateral response across vehicle speed/velocity. It is therefore suggested as a possible control specification and not an optimum value established in the experiment. The schedule is designed to play it safe below 40 km/h, opting for a higher road-wheel angle, up to 35°, and a longer turn radius, 3.86 m at rest. For the same vehicle geometry and within the kinematic approximation, increasing road-wheel steering angle decreases turning radius.

3.8 Tremor filter response and latency budget

Table 8. Second-order Butterworth attenuation at both scheduled cutoffs.

Input frequency	Clinical association	Attenuation at f_c = 3 Hz (≤30 km/h)	Attenuation at f_c = 6 Hz (≥80 km/h)
1 Hz	Voluntary steering	−0.05 dB (99.4% passed)	−0.00 dB (100.0%)
2 Hz	Voluntary steering, upper bound	−0.78 dB (91.4%)	−0.05 dB (99.4%)
3 Hz	Cerebellar/intention tremor, lower bound	−3.01 dB (70.7%)	−0.26 dB (97.0%)
4 Hz	Parkinsonian rest, essential tremor	−6.19 dB (49.0%)	−0.78 dB (91.4%)
6 Hz	Parkinsonian rest, upper bound	−12.30 dB (24.3%)	−3.01 dB (70.7%)
8 Hz	Essential, physiological tremor	−17.12 dB (13.9%)	−6.19 dB (49.0%)

Input frequency	**Clinical association**	**Attenuation at f_c = 3 Hz (≤30 km/h)**	**Attenuation at f_c = 6 Hz (≥80 km/h)**
10 Hz	Physiological tremor	−20.95 dB (9.0%)	−9.40 dB (33.9%)
12 Hz	Physiological tremor, upper bound	−24.10 dB (6.2%)	−12.30 dB (24.3%)

At the low-speed cutoff, the filter passes over 91% of voluntary input at 2 Hz while rejecting 76–94% of the 6–12 Hz band. The 3–4 Hz region is the weak point: only 51% of a 4 Hz input is rejected by the low-pass alone, which is precisely why the adaptive notch is specified. With the notch delivering its target ≥20 dB at the tracked dominant peak, combined rejection at 4 Hz reaches −26 dB (5% passed).

Table 9. End-to-end input latency budget against a 150 ms ceiling.

Stage	**Low speed (f_c = 3 Hz)**	**High speed (f_c = 6 Hz)**	**Basis**
Sensor acquisition and ADC	4 ms	4 ms	500 Hz sampling, two-sample settle
Median-of-5 outlier rejection	4 ms	4 ms	(N−1)/2 samples at 500 Hz
Deadzone and rate limiter	1 ms	1 ms	Single cycle
Butterworth low-pass group delay	75 ms	37 ms	$\tau = \sqrt{2}/(2\pi f_c)$
Adaptive notch, off-band	8 ms	8 ms	Specified budget
CAN-FD frame and arbitration	10 ms	10 ms	10 ms worst-case cycle
Steering actuator closed-loop rise	40 ms	40 ms	Typical EPS response
Total	142 ms	104 ms	vs ≤150 ms ceiling
Distance travelled during delay at the highest speed each setting applies	1.18 m (30 km/h)	2.89 m (100 km/h)	v × t

The distance row is added since it is the most direct representation of the cost. The filter that makes the console usable for a driver with tremor also introduces a lag equivalent to about 2.9 m of travel at 100 km/h, roughly two-thirds of a typical car length. This is the main unresolved trade-off in the design, and it is discussed in Section 4.5.

3.9 Consolidated design specification

The ultrasonic subsystem is called out as a low speed manoeuvring aid and is not intended to be a general forward-collision avoidance system at normal road speed. The proposed sensing range and alert thresholds are therefore for parking and low speed manoeuvring conditions. The 3 alert thresholds are tentative interface design goals. These should not be taken as validated thresholds for stopping distances as no user reaction-time study has been done.

Table 10. Derived design targets, with derivation basis and confidence.

Parameter	Unit	Conventional baseline	Iteration 2 target	Derivation basis	Confidence
Steering angular range	deg	±450 (900 lock-to-lock)	±25	Figure 2 annotation; 18:1 angular compression	Design fixed
Steering gain	°/°	~0.067 (15:1 ratio)	1.40 → 0.09, speed-scheduled	Section 2.6, Table 6	Derived, untested
Full-deflection lateral acceleration	g	≈0.8–0.9 at the tyre–road limit, dry asphalt (Gillespie 1992)	0.46–0.48 above 40 km/h	Bicycle model, L = 2.7 m, K = 0.0024 s²/m²	Derived, untested
Minimum turn radius, at rest	m	~3.9 (35° road wheel)	3.86	L/tan δ	Derived
Joystick breakout force	N	2–4 N·m rim torque	3–5 (steering), 5–8 (trigger)	Set below reported tenodesis/pinch capability	Assumed, requires MVC study

Centring stiffness	N·mm/deg	n/a	12–45, profile-adjustable	0.09 m grip radius; 3.3–12.5 N at full deflection	Derived
Force-feedback ceiling	N	Absent in reviewed systems	0.40 × F_MVC, envelope 0–15 N	Section 2.8 strength-conflict constraint	Derived, untested
Force-feedback bandwidth	Hz	n/a	≥100 (output path, unfiltered)	Asymmetric filtering rationale, Section 2.7	Design specification
Input deadzone	% of arc	n/a	8–12 (2.0–3.0°)	3–5 mm tremor excursion at 90 mm grip radius	Derived
Sensor resolution	°/LSB	n/a	0.0122 (12-bit over 50°)	50°/4096	Derived
Residual cross-axis coupling	% FS	n/a	≤5 target	Deadzone plus 2 × 2 decoupling matrix	Target — requires bench test
Input latency	ms	~100 (typical EPS)	143 low speed, 105 high speed	Table 8	Derived, untested
Braking deceleration	m/s²	up to ~8	0–8, proportional trigger	ECE R13 expectation referenced for Joysteer 3.0	Standard-derived
Proximity range	m	n/a	0.3–5, ±10 mm, 20 Hz update	Four-sensor 40 kHz ultrasonic array	Component-derived
Proximity alert tiers	m	n/a	2.5 caution / 1.5 warning / 0.8 imminent	Stopping distance at 10 km/h: 0.5 s	Derived

				reaction + 4 m/s² decel = 2.36 m	
Mode-switch time	s	Hours (mechanic-serviced)	4.5 (target <5)	0.6 auth + 0.9 handshake + 1.4 actuator + 1.6 self-test	Budgeted, untested
Fail-safe response	ms	n/a	50	30 detect (3 × 10 ms watchdog) + 15 safe-state + 5 annunciation	Budgeted; requires formal HARA
Stored profiles	count	0 (fixed at manufacture)	5	Fault F5 specification	Design fixed
Operating temperature	°C	−40 to +85	−40 to +85	Automotive-grade component class; no relaxation	Standard
Power consumption	W	n/a	<10 continuous, 25 peak	1.35 N·m per axis, duty-cycled, 12 V supply	Estimated

Table 11. Control-mapping

User/control action	**Vehicle/system function**	**Operating restriction**
Joystick lateral displacement	Steering command	Available in drive mode
Joystick longitudinal command	Acceleration/braking command, according to defined mapping	Available in drive mode
Auxiliary buttons	Secondary vehicle functions	Function dependent
Gear-selection input	P/R/N/D request	Stationary + brake applied + explicit gear mode

Mode-selection control	Change control mode/profile	Locked while vehicle is moving
Emergency control	Initiate defined minimal-risk response	Available continuously

This table defines the proposed command architecture only; it does not represent an experimentally validated control implementation.

Table 12. Preliminary safety requirements and hazard analysis

Hazard/failure	Potential consequence	Proposed design requirement
Joystick sensor fault	Incorrect steering/braking command	Redundant/plausibility-checked sensing; fault-state transition
Filter instability/mistracking	Distorted user command	Bounded parameters and deterministic fallback
Haptic actuator fault	Excessive/resistive force	Force/current limiting; passive/manual command remains available
Unintended mode switch	Unexpected command mapping	Inhibit mode changes while moving
Gear command while moving	Drivetrain/vehicle-state hazard	Zero-speed + brake + explicit-mode interlock
Communication loss	Loss/delay of control command	Fault detection and defined degraded/minimal-risk response
Emergency-control activation	Abrupt loss of authority	Controlled minimal-risk response

3.10 Preliminary safety requirements and hazard analysis

Safety is required as an architectural attribute and not just a reliability attribute, as the proposed console is used for safety-critical functionality. This document is not a formal HARA, FMEA validation or ISO 26262 safety case. Instead, the preliminary hazard-oriented analysis is employed to define design requirements that need to be addressed before prototype implementation.

4. DISCUSSION

4.1 What the coverage result does and does not establish

The proposed console is shown in Table 4, in which 92.9% of capabilities are covered compared to the 28.6% of what exists today for the best-in-class console. That gap is wide and requires careful qualification, as it is comparing two types of objects: shipping products certified, installer networks, and field histories, whereas only a design specification exists.

It's a one-way comparison. It sets the 6 target capabilities as mutually exclusive capabilities found in any of the systems that were reviewed, which is a true reflection of the state of the art. It does not prove that the proposed console is better than any of them, as performance is a characteristic of the hardware built, and this console is not built. Table 4 should not be interpreted as awarding a score, but to illustrate an unoccupied portion of the design space.

The second qualification relates to the evidence base. Based on vendor documentation, coverage scores were assigned for commercial systems. The documentation of a vendor is marketing, with an appendix of specifications; it is a reliable report of what a product does, but it is not a reliable report of what it doesn't. Perhaps Joysteer 3.0 or AEVIT 2.0 does a form of input smoothing which simply isn't documented anywhere. The zeros in Table 4 are not to be interpreted as "shown to be present," but rather as "not evidenced in the reviewed sources”.

4.2 Comparison with the Maya Mobility 4-Way Joystick

The most obvious example of a capability gap is the Maya system, which is not a disagreement on design, but rather it cannot be used. The four-direction constraint will result in quantised steering and speed; there will be no cross-axis coupling problem as in Fault F2 since the continuous control is removed. The proposed console brings back proportional multi-axis control and re-introduces the coupling issue, which is then solved by per-axis sensitivity curves and a decoupling matrix.

This is not a simple upgrade; it's a true trade. Four-direction control is coarser, but it is also inherently capable of resisting tremor in the unused diagonal since off-axis motion will not result in off-axis output. This proposed design introduces proportional control and compensates for it with the addition of a filtering subsystem, a 143 ms delay, and a calibration procedure, which is not required for the Maya system. Whether the exchange is advantageous to the user or not is a question that a comparative trial would address.

4.3 Comparison with Joysteer 3.0

In Table 3, Joysteer 3.0 is the strongest of all of the existing systems. It is not a temporary lack; it's the completed programme of type approval of steering equipment, braking, and electromagnetic compatibility, which includes ECE R79 Annex 6 for complex electronic vehicle control systems.

All the claimed benefits of the proposed console (adaptive profiling depth, tremor filtering, proximity sensing and open calibration) are software and sensing improvements that are “upstream” of exactly the safety case addressed by Annex 6. The introduction of an adaptive filter to a steering input path is not a neutral addition with respect to the certification: it adds a transfer function that is user-configurable and depends on the state of the system, which is difficult to argue compared to a fixed transfer function. The right answer is that the console that is proposed trades capability for certification tractability, and the price of the trade is not yet known.

These are limitations that Joysteer's reported limitations can be attributed to: high cost, specialist-only installation, complex setup. It is not demonstrated here that they can be delivered while meeting the same regulatory burden.

4.4 Comparison with EMC AEVIT 2.0

AEVIT 2.0's flash-upgradeability is more iterative than anything else, and its joystick and touchscreen setup looks forward to the digital status screen of Iteration 2. The differences are only architectural, not functional, because AEVIT's proprietary, vehicle-specific integration is the root cause of its lack of installers and its price, and the proposed design goes after that model, not after its features.

There's a counterargument that needs to be made. Proprietary integration of the vehicle is more than just a business approach; it is a way to enclose the safety argument. A defined vehicle set is a system that can make assumptions that a universal system cannot make. The proposed ‘universal mounting bracket and open calibration interface' is claimed in Fault F7's fix, but is not clearly defined as part of a CAN signal set, a vehicle compatibility matrix, or an installer competency standard. The proposed console is not an architecture, as is the case with AEVIT.

4.5 Comparison with J4D and the HFES-Europe findings, and the answer to RQ1

RQ1 investigated the possibility of adding force feedback and tremor filtering without reverting to the fatigue and precision limitation effects reported by J4D and by HFES-Europe. Regarding RQ1, it is illustrated how the speed-dependent gain scheduling, frequency-selective input filtering and user-scaled force feedback can be integrated to a single control architecture. But the present study is neither evidence of improvements in driving precision, fatigue nor usability as these outcomes were not experimented. Thus, the analysis can be used to support architectural feasibility, quantitative design targets, but performance and fatigue effects are yet to be validated.

The cross-talk issue with HFES-Europe is related to the lack of a good gain law and a compressed angular range. This is achievable: Table 6 indicates that the full-deflection lateral acceleration is normalised in this range as a percentage of g, with the results between 0.46 and 0.48, which is a 4.1% spread. This schedule will effectively eliminate the counter-intuitive behaviour, as the stick will be the same thing at 40 km/h as at 120 km/h. This is a more powerful statement than "speed-dependent gain helps" since it specifies which of the invariants should remain unchanged.

The argument on fatigue is less than the design modifications suggest. The mental workload and stress that were experienced during city driving were observed to be high, as noted in J4D. Iteration 2 answers with biomechanical modifications: a travel range of ±25°, a 30% reach loss, wrist-only actuation. These deal with physical effort, and none of the samples in the reviewed corpus show that decreasing physical effort decreases cognitive workload. The plausibility of demanding fine control of a high-authority input in dense traffic, however, is not necessarily connected with arm travel. The suggested console is intended to lessen physical fatigue without affecting the J4D workload.

The filtering process brings a cost to the precision, quantified in Table 8: The input latency is 142 ms at low speed and 104 ms at high speed, equivalent to 1.18 m of travel at 30 km/h and 2.89 m at 100 km/h. The notion of speed-scheduling the cutoff is a coherent one, in that it shifts the burden of the low-pass to where it is least well validated, namely the adaptive notch. When the notch is unable to follow the dominant tremor frequency of the user at speed, it becomes a 6 Hz low-pass filter with a 91% pass-band ratio for a 4 Hz tremor input.

4.6 Comparison with the patent art

The proposed console lacks novelty in the concept, since the concept of force feedback for a disabled driver is considered to be “prior art” as shown in U.S. 7,970,514. Haptic steering guidance is also an established research topic in able-bodied driving (Benloucif et al., 2019; Melman et al., 2017). The delta is subject to two constraints that the patent does not contain.

The first one is the strength-conflict constraint defined in Section 2.8. The force limits of the force feedback provisions in the review are absolute. The absolute ceiling is the wrong specification (15 N of feedback is informative to a user with 100 N, disabling to a user with 20 N), and specifying the ceiling as 0.40 x F_MVC has relatively small consequences for who can use the system. The coefficient of 0.40 is an assumption that needs to be verified.

The second one is asymmetric filtering. If the same low-pass filter that eliminates tremor from the input signal was also applied to the feedback output, the road surface information above 3Hz would be lost – most of the information that the road surface is trying to give is above 3Hz. It is argued that this is the most transferable design feature disclosed in the paper, and it resolves a patent literature (PL) and commercial documents (CD) conflict that is not addressed.

The passive potentiometer-based sidestick of EP 1,595,766 and the hydraulic controller of US 4,722,416 are not compared, but are superseded.

4.7 The gear-integration question and the answer to RQ2

RQ2 concerned the effect of combining gear selection with the joystick on the risk of incorrectly interpreting the gear state. The evidence is actually split and cannot be declared or said to be settled.

However, even if these designs were shown to have higher measured error rates than the designs they defeated, participants preferred joystick-type selectors over button, rotary, and stalk designs, against

integration. Preference and performance are not correlated, and in a task that is used in a safety-critical setting, performance is the metric that is relevant. The danger of mode confusion is inherent with incorporating another gear function onto a control that is already used continuously for steering and speed control, which is not the case with separate selectors.

It has been linked to rotary and touchscreen selectors, which were used to eliminate tactile feedback of the positioning operation to achieve a more compact design, and 1,448 NHTSA rollaway reports on a total of 684 crashes or fires, none of which proved fatal, but for which the investigation was closed without a defect being identified. What those designs have in common is the absence of a physical gear-shift feedback rather than the use of a joystick. If the driver is unable to access the traditional lever, he or she might have a single-hand option that is an integrated joystick selector.

Table 5 dispenses with this and gives a conditional answer. Joystick-type selection is still level overall with the mechanical lever (the mechanical lever is 3.80 under accessibility-weight, and the joystick is 3.80 under it). If the tactile deficit is not corrected, there is no justification for integration because operability is a disqualifying characteristic of the desired population and error rate is a design feature. The score is increased to 4.45 with the added haptic detents for each gear and required display confirmation.

Experience with electronic gear selectors shows that gear-state confusion does not occur only with rotary and touchscreen gear selectors. The monostable spring-return electronic selectors are also an important precedent as the physical selector can return to a common position after receiving a gear command, which means that the lever position itself does not indicate the current gear state (Lohilahti Bladfält et al. 2020). Accordingly, the present study does not presume that the integration of gear selection into a joystick automatically will decrease gear-selection error.

Therefore, gear-state safety is considered as an interface requirement of the system and not dependent on the form factor of the joystick for the proposed console. Persistent visual feedback of engaged gear, tactile/haptic feedback of gear selection commands accepted, and an interlock to prevent gear selection commands when the vehicle is moving would be required by the proposed design. Selection of gears is only allowed when the vehicle is stopped, the service brake is applied and the driver has purposely entered into the gear selection mode.

The present analysis does not show that the proposed selector would result in fewer selection errors than a rotary, push-button, column-mounted or other electronic selectors because the proposed selector has not been physically implemented or evaluated with users. RQ2 is therefore answered conditionally: Gear selection is technically possible to be integrated into the accessible-control interface, but has to be explicitly confirmed by the user, mode separation is required, and interlocks should be used for safety; however, the comparative error rate has to be validated by experimentation.

The analysis does not prove that the joystick-integrated gear selection has any lower inherent error risk as compared to a rotary, push-button, column or other electronic selectors. Rather, the evidence suggests gear-state ambiguity is highly dependent on the visibility of the states, confirmation of commands, interface behaviour and interlocks. The proposed integration is thus only proposed as a conditional design

option that needs to be indicated as persistent, distinctive feedback, stationary vehicle selection, brake interlocking, and empirical testing in the future.

4.8 Complexity as a safety variable

Table 5 is more than just about transmissions. The single-speed architecture is the least efficient at highway speeds, but reliability and complexity combined are only 0.45 of the weight; simplicity is the winner. That's not enough to offset the 4% to 15% increase in efficiency that multi-speed models can offer (Ruan et al. 2018) .

This is not a desirable effect when used directly on a console. The proposed design is added to a control path where the user's stopping ability is dependent. Each add-on is a reliability cost, and the user who can't revert to manual control can't afford to fail more than would an able-bodied driver, by its own weighting criteria. Before prototyping, therefore, the tension between the gearbox conclusion and console specification in the paper is resolved, which likely involves determining the failure modes of which subsystems must be fail-operational instead of simply fail-safe. Adding adaptive filtering, active haptics, profile storage, mode logic, proximity sensing, and integrated gear selection adds to the number of potential failure modes and interaction points. Complexity is thus considered as a safety factor within the current architecture. The functions are segregated based on safety criticality, the adaptive algorithms are limited to deterministic fallback behaviour, mode transitions are interlocked and auxiliary functions are not allowed to jeopardize the primary steering/braking command path. The requirements are not a validated safety architecture, but constraints to be considered when implementing a safety architecture.

4.9 Limitations and threats to validity

Construct validity. Capability absences are based on vendor-documented evidence as described in Section 4.1. The 23 candidates were consolidated to 8 faults, but the consolidation is not reported and not reproducible by another analyst.

Internal validity. All the performance numbers in Tables 7-10 are analytically calculated, not measured. The linear regime is assumed in the bicycle model and is the range where the 0.46–0.48 g normalisation applies. Since the evaluation of Butterworth group delay is done at DC, the values of the latency from Table 9 are optimistic for frequencies near the cutoff. The 2 Hz voluntary-input bound and the tremor frequency bands are chosen from the literature.

External validity. None of the users who have tremors, spasticity, or quadriplegia have tested any aspect of this design. The target population is also diverse, and a five-profile store is an assumption about that diversity, not a fact.

Evidence quality. The gearbox and selector sections are based on secondary sources. There are currently a few references to ResearchGate mirrors instead of original venues, and the primary write-up of J4D is not found.

Weighting. A priori weights for rubrics were used and are also a judgement. Another methodological drawback is that one analyst coded the evidence and scored it for comparison. This means that the interpretation may have been subjective, which could have led to some individual classifications. Independent replication of the coding and formal inter-rater agreement should be included in future extensions of the review.

5. CONCLUSION

This paper reviewed three commercial single-lever driving controls, three research systems and four patent families, and concluded that six capabilities relevant to drivers with tremor, spasticity, or quadriplegia, namely adaptive per-user profiling, tremor filtering, active force feedback, proximity sensing, rapid mode switching, and fatigue-reducing ergonomics, are all represented separately in the corpus but not together. A design space comparison was used to compare the literature reviewed with the systems in this study, showing that the design space is fragmented with some of the reviewed systems only addressing parts of the accessibility, filtering, feedback, adaptation and interface requirements considered. All these requirements are incorporated into the proposed architecture as part of the design specification, but their presence in the design specification does not show how effective they are in an actual implementation.

Eight consolidated faults were derived and mapped one-to-one onto design fixes, which were also carried forward from Iteration 1 to Iteration 2 through six quantifiable changes: a travel arc limited to a maximum of ±25°, a 30% reduction in reach of the auxiliary buttons, a recessed, guarded emergency stop, a haptic indicator ring, a status display of 40 × 20 mm, and a mounting bracket widened by 60 mm in total span. The display resides in the unchanged 45 mm body height, making for no dimensional regression.

Three analysis results are provided that can be used independent from this console. To find the right normalizing gain, first, an exponentially speed-scheduled steering gain of 1.40 - 0.09 °/° is normalised and sets the full-deflection lateral acceleration to 0.46 - 0.48 g between 40 - 120 km/h, revealing the normalising gain that gain scheduling should maintain. Second, the filtering in an assistive control path needs to be asymmetric; for example, a 3-6 Hz input cutoff, with a 100 Hz output cutoff in the feedback, because a symmetric filter would eliminate the road information that the feedback is meant to provide. Third, instead of establishing absolute force feedback ceilings, the ceiling should be based on actual user capability (F_MVC) because absolute ceilings eliminate the users for which the system is being designed.

Hidden costs are not included in the stated costs. The input latency is 143ms at low speed for filtering. Each subsystem added is a reliability cost on a control path that may not allow the user to switch back to manual control. Gear integration is enabled only under certain conditions, and only if dented tactile confirmation is enabled.

In this paper, no measurements have been taken. The contribution is a specification that can be traced and is an explicit statement of trade-offs, not a proof of performance.

6. FUTURE PERSPECTIVES

6.1 Bench validation of the filter cascade. Record tremor signals from clinical populations and inject these signals into the input path, and measure the level of attenuation and the latency compared to Tables 8 and 9. Before any vehicle integration, set up a fallback behaviour for adaptive-notch tracking loss.

6.2 Maximum voluntary force study. These are assumed to be the 0.40 x F_MVC coefficient and the 3-8 N breakout thresholds. Before specification lock, a grip-force study across C5–C7 tetraplegia, essential tremor, and spastic presentations is needed.

6.3 Hardware-in-the-loop verification of the gain schedule. The lateral-acceleration normalisation in Table 7 must be checked in a validated vehicle model, using non-linear tyres, before it is used on the road; otherwise, the bicycle model is no longer valid at the adhesion limit. Hardware-in-the-loop evaluation should quantify end-to-end latency, gain-schedule transitions, filter stability, notch-tracking behaviour, sensor-fault detection, mode-transition interlocks, communication faults, and minimal-risk responses under reproducible simulated driving conditions.

6.4 User trials. To test whether or not the biomechanical changes in Iteration 2 impact the cognitive workload finding that J4D reported, follow the example of the 16-driver on-road study (PETERS and OESTLUND 2026) and include the cognitive workload instrumentation (NASA-TLX or equivalent). A follow-up study is needed to compare the proposed adaptive configuration with a fixed gain/no haptic counterpart. The participants should reflect the actual population of people who could benefit from using the accessible driving system and they should be stratified if possible by the relevant upper-limb motor characteristics. Path-tracking error, unintended-command frequency or errors, task completion time, subjective workload, fatigue/discomfort rating, and mode/gear-selection errors are examples of primary outcomes to be considered. Sample size ought to be established beforehand based on the selected primary outcome and an appropriate power analysis, and not just chosen arbitrarily.

6.5 Detented gear-selection prototype. *C*onstruct and compare the haptic-detent selector with rotary and push-button baselines on error rate and not preference, the latter of which is the basis of Table 6.

6.6 Certification pathway analysis. Analyze the safety case for ECE R79 Annex 6 for a user-configurable, state-dependent transfer function in a steering input path and complete an ISO 26262 HARA to determine and/or update the 50ms fail safe budget.

6.7 Cost verification. Get vendor quotes for Joysteer 3.0 and AEVIT 2.0 installation. There is currently no evidence of a cost claim in Fault F7.

6.8 Complexity audit. Resolve the tension described in Section 4.8 by determining the fail-safe/fail-operational classification of each subsystem, and eliminating those that are not justified in terms of reliability cost.

Acknowledgements: The author thanks Arbaz Reza for supervision and review throughout the design iterations.

Technical and data sources: manufacturer documentation from Maya Mobility, Steering Developments, and Electronic Mobility Controls; ONCE Foundation and Universitat Politècnica de València (J4D Project); VTI and the DiVA Portal.

REFERENCES

Benloucif, M. A., C. Sentouh, J. Floris, P. Simon, and J. C. Popieul. 2019. 'Online Adaptation of the Level of Haptic Authority in a Lane Keeping System Considering the Driver's State'. *Transportation Research Part F: Traffic Psychology and Behaviour* 61 (February): 107–19. https://doi.org/10.1016/j.trf.2017.08.013.

Bhatia, Kailash P., Peter Bain, Nin Bajaj, et al. 2017. 'Consensus Statement on the Classification of Tremors. From the Task Force on Tremor of the International Parkinson and Movement Disorder Society'. *Movement Disorders* 33 (1): 75–87. https://doi.org/10.1002/mds.27121.

Bhidayasiri, Roongroj, Suppata Maytharakcheep, Saisamorn Phumphid, and Walter Maetzler. 2022. 'Improving Functional Disability in Patients With Tremor: A Clinical Perspective of the Efficacies, Considerations, and Challenges of Assistive Technology'. *Journal of the Neurological Sciences* 435 (April): 120197. https://doi.org/10.1016/j.jns.2022.120197.

Bhise, Vivek D. 2011. *Ergonomics in the Automotive Design Process*. https://ftp.idu.ac.id/wp-content/uploads/ebook/ip/BUKU%20ERGONOMI/BUKU%20INGGRIS/Ergonomics%20in%20the%20Automotive%20Design%20Process.pdf.

El-Sheikh, Amira F, Alaa B Hassan, and Nanees E Mohamed. 2025. 'Effect of Leg Pedaling Exercise From an Inclined Position on Functional Ability and Strength in Children With Diplegia'. *Journal of Taibah University Medical Sciences* (Saudi Arabia) 20 (1): 73–80. PubMed Central. https://doi.org/10.1016/j.jtumed.2025.01.001.

Electronic Mobility Controls. 2022. 'AEVIT™ 2.0 System Overview'. April 21. https://electronicmobilitycontrols.com/products/system-overview/.

Gillespie, Thomas D. 1992. *Fundamentals of Vehicle Dynamics*. (Warrendale, PA), ahead of print, February. https://doi.org/10.4271/r-114.

Lacock, Stephan, Armand André du Plessis, and Marthinus Johannes Booysen. 2023. 'Electric Vehicle Drivetrain Efficiency and the Multi-Speed Transmission Question'. *World Electric Vehicle Journal* 14 (12): 342. https://doi.org/10.3390/wevj14120342.

Lenka, Abhishek, and Joseph Jankovic. 2021. 'Tremor Syndromes: An Updated Review'. *Frontiers in Neurology* (Switzerland) 12 (July): 684835. PubMed Central. https://doi.org/10.3389/fneur.2021.684835.

Li, Zihong, Hangyu Lu, Ning Zhang, Hongliang Wang, and Dawei Pi. 2026. 'Stability and Gain Analysis of a Robust Steering Control System for a Corner Module With Hybrid Time Delay'. *Journal of Vibration and Control*, ahead of print, September 29. https://doi.org/10.1177/10775463261481156.

Lohilahti Bladfält, Sanna, Camilla Grane, and Peter Bengtsson. 2020. 'Comparison of Usability Between Gear Shifters With Varied Visual and Haptic Patterns and Complexities'. *Multimodal Technologies and Interaction* 4 (2): 24. https://doi.org/10.3390/mti4020024.

Melman, T., J. C. F. de Winter, and D. A. Abbink. 2017. 'Does Haptic Steering Guidance Instigate Speeding? A Driving Simulator Study Into Causes and Remedies'. *Accident Analysis & Prevention* 98 (January): 372–87. https://doi.org/10.1016/j.aap.2016.10.016.

Mo, Jiancheng, and Ronny Priefer. 2021. 'Medical Devices for Tremor Suppression: Current Status and Future Directions'. *Biosensors* 11 (4): 99. https://doi.org/10.3390/bios11040099.

PETERS, B, and J OESTLUND. 2026. 'Joystick Controlled Driving for Drivers With Disabilities: A Driving Simulator Experiment'. *VTI Rapport*, no. 506A. https://trid.trb.org/View/772213.

Rollover Data Special Study: Final Report. 2011. DOT study. U.S. Department of Transportation, National Highway Traffic Safety Administration.

Ruan, Jiageng, Paul D Walker, Jinglai Wu, Nong Zhang, and Bangji Zhang. 2018. 'Development of Continuously Variable Transmission and Multi-Speed Dual-Clutch Transmission for Pure Electric Vehicle'. *Advances in Mechanical Engineering* 10 (2). https://doi.org/10.1177/1687814018758223.

Ruan, Jiageng, Paul Walker, and Nong Zhang. 2016. 'A Comparative Study Energy Consumption and Costs of Battery Electric Vehicle Transmissions'. *Applied Energy* 165 (March): 119–34. https://doi.org/10.1016/j.apenergy.2015.12.081.

Steering Developments. 2026. 'Joysteer 3.0 Electronic Driving System'. Steeringdevelopments.Co.Uk. https://steer-bright-start.lovable.app/products/joysteer-electronic-driving-system.

Wada, Masayoshi, and Fujio Kameda. 2009. 'A Joystick Car Drive System for Wheelchair Users'. *2009 International Conference on Mechatronics and Automation*, August, 921–25. https://doi.org/10.1109/icma.2009.5246335.